Molecular Vision 2023; 29:58-67 <http://www.molvis.org/molvis/v29/58>
Received 9 November 2022 | Accepted 18 May 2023 | Published 20 May 2023

Basement membrane regeneration and TGF-β1 expression in rabbits with corneal perforating injury

Na Meng, Jinling Wu, Jingjing Chen, Yuqing Luo, Luxing Xu, Xia Li

Department of Ophthalmology, The First Affiliated Hospital of Guangxi Medical University, Nanning, China

(The first two authors contributed equally.)

Purpose: To evaluate the relationship between basement membrane (BM) regeneration and the spatiotemporal expression of TGF-β1 during wound healing in rabbits with corneal perforating injury.

Methods: Forty-two rabbits were randomly allocated into 7 experimental groups, with 6 rabbits per group at each time point. The central cornea of the left eye was injured with 2.0 mm trephine to establish the perforating injury model. Six rabbits that received no treatment were used as controls. The cornea was evaluated at 3 days, 1–3 weeks, and 1–3 months after injury with a slit lamp for haze levels. Real-time quantitative polymerase chain reaction (qRT-PCR) was performed to quantify the relative expression of TGF-β1 and α-SMA mRNA. Immunofluorescence (IF) was used to assess TGF-β1 and alpha-smooth actin (α-SMA) expression and localization. BM regeneration was assessed using transmission electron microscopy (TEM).

Results: After injury, dense haze appeared at 1 month and then gradually faded. The relative expression of TGF-β1 mRNA peaked at 1 week and then decreased until 2 months. The relative α-SMA mRNA expression reached its peak at 1 week, then reached a small peak again at 1 month. IF results showed that TGF-β1 was initially detected in the fibrin clot at 3 days and then in the entire repairing stroma at 1 week. TGF-β1 localization gradually diminished from the anterior region to the posterior region at 2 weeks to 1 month, and it was nearly absent at 2 months. The myofibroblast marker α-SMA was observed in the entire healing stroma at 2 weeks. Localization of α-SMA gradually disappeared from the anterior region at 3 weeks to 1 month, remaining only in the posterior region at 2 months and disappearing at 3 months. Defective epithelial basement membrane (EBM) was first detected at 3 weeks after injury, then gradually repaired, and was nearly regenerated at 3 months. A thin and uneven Descemet's membrane (DM) was initially detected at 2 months after injury, then gradually regenerated to some extent, but remained abnormal at 3 months.

Conclusions: In the rabbit corneal perforating injury model, EBM regeneration was observed earlier than DM. At 3 months, complete EBM regeneration was observed, while the regenerated DM was still defective. TGF-β1 was distributed throughout the entire wound area in the early stages and then decreased from the anterior to the posterior region. α-SMA exhibited a similar temporospatial expression to TGF-β1. EBM regeneration may play a key role in low expression of TGF-β1 and α-SMA in the anterior stroma. Meanwhile, incomplete DM regeneration may contribute to the sustained expression of TGF-β1 and α-SMA in the posterior stroma.

Penetrating ocular trauma is commonly observed during clinical practice. It has been established that corneal penetrating injury frequently causes corneal scarring, which results in irregular astigmatism and vision impairment [1]. Growing evidence suggests that corneal basement membranes (BMs) are critical regulators of corneal fibrosis [1-4]. The two main BMs of the cornea, the epithelial basement membrane (EBM) and Descemet's membrane (DM), are reportedly damaged during corneal penetrating injury [5]. Given that most emphasis has been placed on the regeneration of the BM during corneal refractive surgery in animal models, little is known about the regeneration of EBM and DM during corneal penetrating injury.

TGF-β1 is an essential growth factor in corneal stromal fibrosis [6-9]. TGF-β1 can transform corneal keratocytes into opaque myofibroblasts, which produce and deposit a huge amount of disorganized extracellular matrix, resulting in stromal scarring and corneal opacity [10-12]. Damaged EBM could allow TGF-β1 to persistently permeate into the stroma from the tear fluid and epithelium, driving myofibroblast growth and maintenance, while EBM regeneration could limit the entry of TGF-β1 into the stroma [1,2,13-15]. An increasing body of evidence suggests that the regeneration of EBM takes several months [16-18]. Accordingly, rabbit corneal perforating injury models were established to evaluate corneal wound healing, the regeneration of EBM and DM, and the spatiotemporal expression of TGF-β1 and α-SMA,

Correspondence to: Xia Li, Department of Ophthalmology, The First Affiliated Hospital of Guangxi Medical University, Nanning, 530021, China; Phone: +867715333710; FAX: +867715333710; email: lixiagmu066@163.com

to investigate the cornea's ability to maintain transparency during the healing process and to identify long-term factors associated with scarring.

METHODS

Animals: All experiments were performed in strict accordance with the tenets of the Association for Research in Vision and Ophthalmology (ARVO) for the Use of Animals in Ophthalmic and Vision Research. The animal study protocol was approved by the Medical Ethics Committee of the First Affiliated Hospital of Guangxi Medical University (Approval Number: 2022-E393–01). Forty-two New Zealand white rabbits, aged 3 months and weighing 1.5 to 2.0 kg, were allocated into 7 experimental groups at random (6 rabbits per group). Six rabbits that received no treatment were used as controls.

Corneal perforating surgery and tissue preparation: The corneal perforating wound healing models in rabbits were established following Connon et al. [19]. Before surgery, tropicamide phenylephrine eye drops were administered to fully dilate the pupil. General anesthesia was introduced by intravenous injection of 1% pentobarbital sodium (3 ml/kg) into the ear edge vein of the rabbits. Topical proparacaine hydrochloride 0.5% was applied to the surgical eyes during the procedure. A 2 mm diameter full-thickness button of the left central cornea in the injury model was injured with 2.0 mm trephine. Within 20 min post-injury, a fibrin clot developed in the wound site, which enabled the anterior chamber to heal.

An overdose of 1% sodium pentobarbital solution was used to euthanize the rabbits. The corneoscleral rims of the rabbits' corneas were removed with micro-dissecting scissors. The corneal tissues were trimmed, and 0.5 mm of normal tissue was left around the wound. The corneas were cut along the equator using a razor blade. One half was preserved in 3% glutaraldehyde for transmission electron microscopy (TEM), and the other was fixed in 4% paraformaldehyde at 4 °C for an overnight period before being dehydrated and embedded in paraffin block. Sections of 5 µm were produced and stored for the immunofluorescence assay.

Corneal opacity and haze grading: A slit lamp examination was performed on day 3, weeks 1, 2, and 3, and months 1, 2, and 3 to analyze the degree of corneal opacity after perforating injury. Corneal haze was scored using the Fantes grading scale [20]. Grade 0 represented a cornea that was completely transparent, grade 0.5 was faint haze with careful oblique illumination by a slit lamp, grade 1 had more prominent haze not interfering with visibility of fine iris details, grade 2 represented a mild obscuration of iris details, grade 3 represented a moderate obscuration of the iris and lens, and grade 4 was severe dense haze with no view of the iris.

Immunofluorescence staining: IF was performed on each cornea at least three times. The paraffin-embedded cornea slices were dewaxed in xylene and rehydrated through a declining ethanol series. After rehydration, the slices were immersed in 3% EDTA and heated in a microwave oven for antigen retrieval. Slices were washed in 0.1 m phosphate-buffered saline (PBS) after being cooled down naturally and permeabilized with 0.3% TritonX-100 at room temperature for 10 min. To avoid possible non-specific binding places, slices were treated in PBS with 5% normal goat serum for 45 min. The slides were then incubated for 12 h at 4 °C with TGF-β1 primary antibodies (GeneTex, GTX21279) and an anti-alpha-smooth muscle actin primary antibody (Abcam, ab7817) diluted 1:100 in 1% BSA. Following three 15 min rinses in PBS, slices were stained for 30 min at room temperature with a 1:200 dilution of the secondary antibodies Alexa Fluor™ 488 (Invitrogen) goat anti-mouse IgG (H + L) in 1% BSA. All sections were counterstained with DAPI for nuclear staining after three PBS washings. Finally, coverslips were used to mount the slides. Negative controls were included without primary antibodies in each assay. Digital images were captured using a confocal laser scanning microscope.

Transmission electron microscopy: The TEM specimens were prepared following the procedures outlined by Fantes et al. [20]. Pieces of cornea tissue were immediately fixed in a solution of 2.5% glutaraldehyde and 4% paraformaldehyde for at least 2 h. Following three 10 min PBS rinses, the specimens were post-fixed in 1% osmium tetroxide for 2 h at 4 °C. Following fixation, the corneas were dehydrated in an increasing series of ethanol concentrations and acetone before being embedded in an epoxy resin medium. Glass knives were used to slice one-micron-thick sections, which were subsequently dyed with 1% Toluidine Blue for orientation of the wound area with light microscopy. The corneal ultrastructure was detected using a transmission electron microscope (Hitachi, Japan). The experiments were performed three times independently and yielded similar results.

Quantitative real-time PCR: Three 3 mm diameter full-thickness plugs of the central cornea tissues were removed and combined at each time point and then immediately preserved in a −80 °C freezer. Corneas were homogenized on ice in 1.5 ml centrifuge tubes containing the lysis buffer R-I. Following the kit's instructions, total RNA was extracted using the AXYGEN reagent kit. In three independent experiments, total extracted RNA was reverse-transcribed into cDNA using the Thermo Scientific RevertAid Reverse Kit. Real-time quantitative polymerase chain reaction (qRT-PCR)

was performed using FastStart Universal SYBR Green Master (ROX). The PCR primer pairs were synthesized as follows: TGF-β1, AGC TGT ACA TTG ACT TCC GCA AGG (forward) and CAG GCA GAA GTT GGC GTG GTA G (reverse); α-SMA, GTT GAC TGA GGC ACC GCT GAA C (forward) and AGT TGT ACG TCC AGA GGC ATA GAG G (reverse). The cycle threshold (Ct) value was recorded, and the 2− ΔΔCT method was used to determine relative gene expression levels.

Analytical statistics: SPSS 22.0 was used to conduct the analytical statistics. Data are presented as the mean ± standard deviation (SD). Significant differences between groups were determined using a one-way ANOVA with the Student–Newman–Kewls method or LSD-t corrected post hoc analysis. A p value <0.05 represents statistical significance.

RESULTS

Corneal opacity: Representative slit lamp photographs of the rabbits' corneas are shown in Figure 1A. After perforating injury, a mild corneal haze first appeared at 3 days and gradually developed into a dense haze by 1 month. At 2 to 3 months after injury, corneal opacity was somewhat alleviated but still present (Figure 1B).

Quantitative real-time PCR: As expected, TGF-β1 was expressed in normal corneas. TGF-β1 mRNA expression was significantly increased 3 days after injury, then continued to increase gradually, peaking at 1 week before gradually decreasing until 3 months. At 1 to 2 months, TGF-β1 mRNA expression was increased and maintained relatively high levels (Figure 2A). Consistent findings were observed for the expression of α-SMA mRNA, as shown in Figure 2B.

Immunofluorescence assay: The immunofluorescent staining of TGF-β1 protein during the wound healing process is shown in Figure 3. In the control cornea, TGF-β1 protein was not detected. Three days after injury, TGF-β1 was strongly detected in the acellular fibrin clot. One week after injury, TGF-β1 was localized in the entire healing stroma. Localization of TGF-β1 gradually diminished from the anterior to the posterior region at 2 weeks to 1 month. One month after injury, TGF-β1 exhibited low expression levels in the posterior region. TGF-β1 was absent in the repairing stroma at 2 to 3 months after injury.

The immunofluorescent staining of α-SMA during the wound healing process is shown in Figure 4. The control cornea had no α-SMA stain detected. Three days after injury, no α-SMA staining was observed. One week after injury, α-SMA expression was found in the anterior region, with dispersed α-SMA expression in the posterior site. At 2 weeks, α-SMA expression was observed in the entire repairing stroma. At 3 weeks to 2 months after injury, α-SMA expression exhibited a decreasing trend from the anterior to the posterior region. Notably, 3 months after injury, α-SMA expression was no longer visible in the posterior stroma.

Transmission electron microscopy: The unwounded (control) corneas exhibited a typical EBM ultrastructure, including the lamina lucida and lamina densa at high magnification (×30,000). After the perforating injury, all corneas at 3 days to 2 weeks exhibited no ultrastructural regeneration of lamina densa or lamina lucida. Three weeks after injury, a nascent defective EBM was first detected, and the lamina densa and lamina lucida of the EBM were irregular and discontinuous. One month after the injury, the EBM ultrastructure was somewhat restored, but its ultrastructure was still uncontinuous. Two months after the injury, the EBM lamina densa and lamina lucida exhibited more continuity than at 1 month, and there were a few discontinuous EBM ultrastructures. Three months after injury, continuous and regular lamina densa and lamina lucida were noted, and the EBM was almost fully restructured (Figure 5).

In the normal cornea, the DM ultrastructure was thick, and a clear boundary was observed even at high magnifications (×10,000). However, DM was not detected until 2 months after injury, when a thin DM appeared in the posterior region adjacent to the nascent endothelium at high magnification (×20,000). Three months after injury, the DM was thicker but remained uneven and loosely attached to the endothelium; the boundary between the DM and stroma remained unclear (Figure 6).

DISCUSSION

It has been established that corneal scarring can reduce the amount of light passing through the cornea to the retina and can cause vision loss [21,22]. Accordingly, understanding the factors involved in the corneal fibrosis repair process is essential for controlling corneal wound healing. Recent studies have found that injured BMs are related to persistent corneal stromal fibrosis, while BM regeneration might be helpful for the resolution of stromal fibrosis [1,23]. Moreover, it is widely thought that regenerated EBM controls TGF-β1 infiltration into the stroma [13,15,24]. TGF-β1 is a well known key fibrotic modulator in mediating the development and maintenance of myofibroblasts [25,26]. Opaque myofibroblasts secrete large amounts of extracellular matrix, resulting in corneal scarring [27,28]. LASIK and PRK animal models have been applied to study corneal fibrosis, but corneal perforation leading to corneal scarring is much more common and severe during clinical practice.

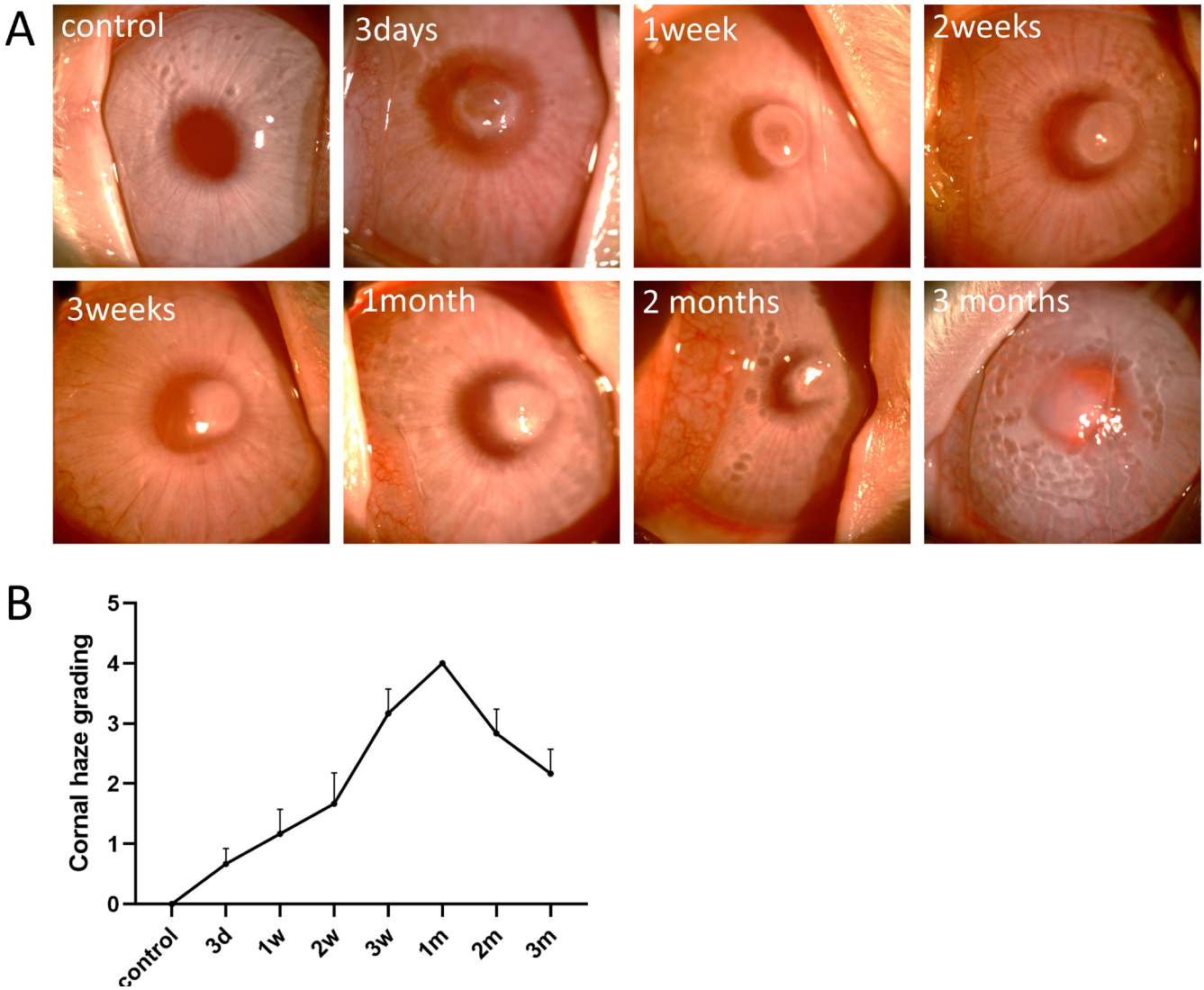

Figure 1. Corneal haze of rabbits. **A**: Slit lamp photographs of rabbit corneal opacity at different time points. Normal unwounded cornea was transparent. Three days after injury, the wound area was filled with translucent fibrous plaques. Fine iris and lens details could be observed 1 week after injury, a prominent haze appeared in the wound margin, and details of the iris could be observed to some extent. Two weeks after injury, increased haze appeared in the wound margin, with mild obscuration of the iris details. Three weeks after injury, a dense opacity appeared in the wound area, with moderate obscuration of the iris details and lens. One month after injury, complete opacification was observed in the wound area, and the iris was not visible. Two months after injury, a focal transparent area appeared in the wound area. Three months after injury, the iris was faintly visible. **B**: Changes in corneal opacity scores at different time points. Corneal opacity appeared at 3 days, then gradually increased, peaking at 1 month before decreasing. The level of corneal haze at each time point after injury was significantly higher than in the control group. The 1 m group exhibited a significantly higher haze score than other groups. Data are expressed as mean ± SD, n=6.

Current evidence suggests that EBM and DM are damaged during corneal perforating injury. In general, 3–6 months are required for corneal repair. However, little is currently known about the changes in EBM, DM, and TGF-β1 during long-term wounding healing, and it remains unclear whether the regeneration of EBM and DM limits TGF-β1 expression in the stroma. Therefore, we investigated BM regeneration and TGF-β1 and α-SMA expression in rabbit corneal perforating injury models for up to 3 months.

The nascent EBM was first detected at 3 weeks after injury and gradually developed until 3 months, when the continuous lamina lucida and lamina densa could be distinguished under TEM. Factors that affect EBM regeneration include the healing of the epithelium, the extent and level

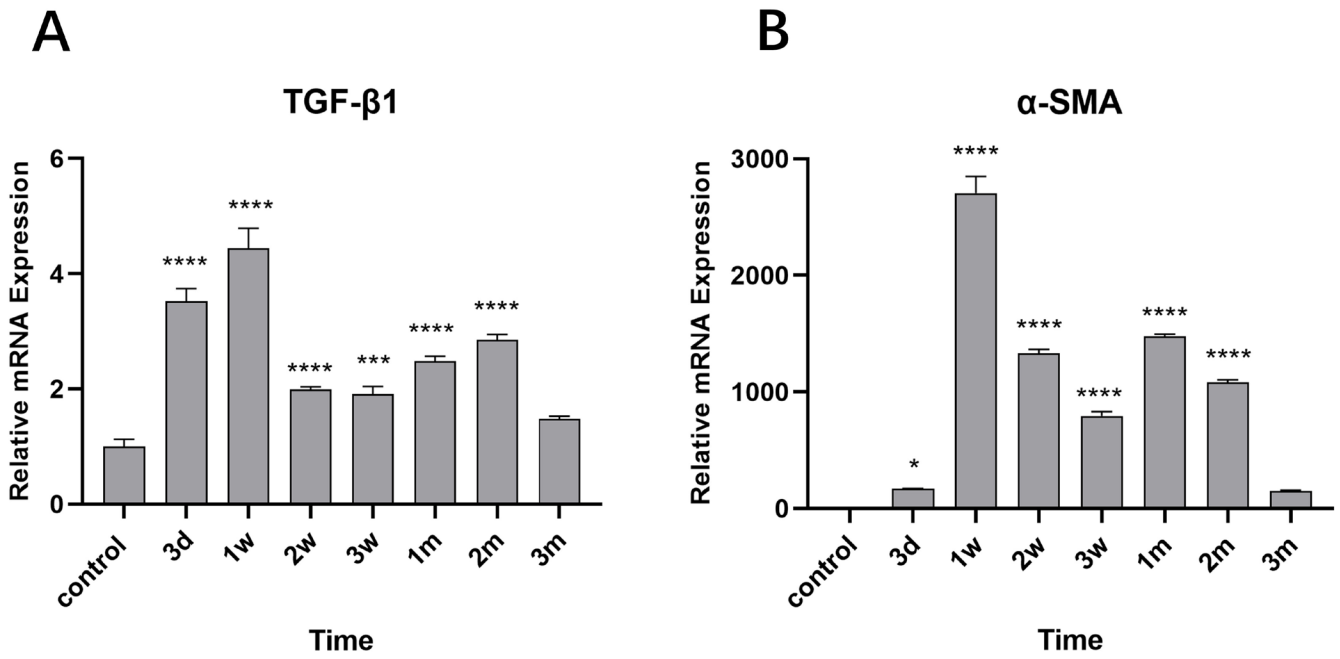

Figure 2. Relative mRNA expression levels in the wound area of the cornea at different time points. **A**: TGF-β1 relative mRNA expression levels. The relative expression of TGF-β1 mRNA was significantly increased at 3 days after injury. Then, relative TGF-β1 expression gradually increased and peaked at 1 week, significantly higher than all other time points before and after injury ($p<0.05$). From 2 to 3 weeks, relative TGF-β1 expression gradually decreased, but then increased again at 2 months and maintained a relatively high level until 3 months. At 3 months, relative TGF-β1 mRNA expression was decreased at 3 months and there was no statistically significant compared to the in normal corneas ($p>0.05$). **B**: α-SMA relative mRNA expression levels. The relative expression of α-SMA mRNA was increased at 3 days after injury. At 1 week after injury, the relative expression of α-SMA mRNA peaked, significantly higher than all other time points before and after injury ($p<0.05$). The relative expression of α-SMA mRNA was downregulated at 2 and 3 weeks, and higher again at 1 and 2 months. At 3 months, the expression of α-SMA mRNA had decreased and was comparable to normal corneas ($p>0.05$). * statistically significant.

of the early stromal keratocyte apoptosis response, and irregularities of the stromal surface after surgery or trauma [5,15,29]. In our perforating corneal model, the corneal epithelium was completely regenerated at 3 weeks, consistent with the literature [30]. This time point is also indicative of the onset of EBM regeneration. In response, the corneal epithelium exhibits laminin synthesis, which can self-polymerize into nascent EBM and subsequently trigger other EBM components, such as nidogens and perlecan, to form mature EBM [31-33].

Severe deficiencies of corneal tissue do not benefit EBM regeneration. Regenerated normal EBM was found in −4.5D PRK rabbit models between 8 and 10 days after surgery, while regenerated EBM was finally detected at 4 months after −9.0D PRK correction. Although the full-thickness central cornea tissue was removed in our model, EBM regeneration was facilitated in the −9.0D PRK model, which may be related to the smaller diameter of the corneal button used in the present study (2 mm) compared to the PRK model (6 mm), suggesting that more keratocytes and corneal fibroblasts around the wound are helpful for EBM component synthesis. Wilson et al. recently confirmed that both keratocytes and corneal fibroblasts can cooperate with the epithelium to regenerate mature EBM [13,23,34,35].

We found that complete EBM regeneration occurred earlier than DM, which was first observed at 2 months after injury and remained defective at 3 months. To date, few studies have focused on DM regeneration. It has been established that DM has poor regeneration potential, and the corneal endothelium may work synergistically with keratocytes to synthesize DM components during this process [3,24,36]. Rabbits' corneal endothelium can proliferate [24], which is not the case for humans [37,38]. The proliferated endothelium and the keratocytes left may be two important factors for DM regeneration. However, more studies are required to understand cell biologic behavior and impact factors.

It has been shown that TGF-β1 plays a prominent role in corneal scarring, as it can promote the transformation of dormant corneal keratocytes into activated fibroblasts and,

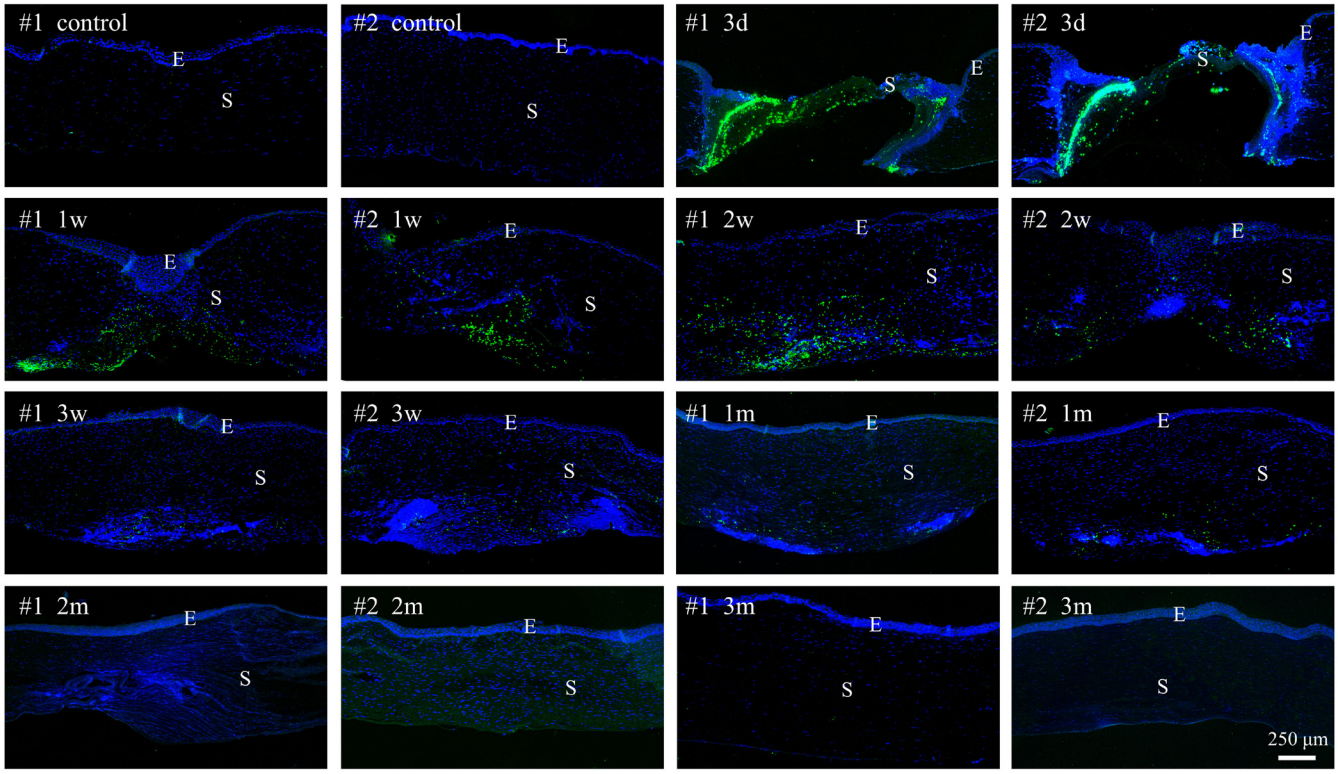

Figure 3. Immunofluorescence staining for TGF-β1 in two different corneas at each time point. In the normal cornea, no TGF-β1 protein was detected in the stroma. At 3 days after injury, a large quantity of TGF-β1 was deposited in the acellular fibrin clot. At 1 week after injury, TGF-β1 was localized to the entire healing stroma. At 2 weeks after injury, the deposition of TGF-β1 had decreased in the anterior stroma, and TGF-β1 was localized to the posterior stroma. At 3 weeks after injury, TGF-β1 was nearly absent in the anterior stroma, and TGF-β1 had decreased in the posterior stroma. At 1 month after injury, TGF-β1 had further decreased, and TGF-β1 was only weakly detected in the posterior stroma. At 2 and 3 months after injury, TGF-β1 was absent in the repairing stroma. Green staining indicates TGF-β1 protein. Blue is DAPI staining of cell nuclei. (E) is the epithelium. (S) is the stroma. Magnification: ×100. Scale bar: 250 μm.

eventually, into differentiated myofibroblasts [6,39-41]. α-SMA is an important marker of fibrosis. In our models, we found that the mRNAs of both TGF-β1 and α-SMA were highly expressed at 1 week after injury. TGF-β1 was detected in the entire wound region at 1 week after injury, and TGF-β1 expression in the anterior stroma started to diminish at 2 weeks after injury. At the same time, α-SMA started to decrease in the anterior region at 3 weeks after injury. α-SMA gradually decreased from anterior region to posterior at 3 weeks to 2 months. These results validated the regulatory effect of TGF-β1 on fibrosis in this corneal perforating injury model.

After the injury, TGF-β1 and α-SMA expression gradually diminished from the anterior corneal stroma to the mid stroma, while slit lamp examination revealed that corneal opacity gradually faded. This corneal scar regression may benefit from the decreased expression of TGF-β1 and α-SMA in the anterior stroma. The anterior EBM was fully regenerated. However, TGF-β1 and α-SMA expression persisted in the posterior region, and the regeneration of DM was delayed and defective. The mRNA expressions of TGF-β1 and α-SMA showed a second peak at 1 to 3 months after injury, which might be responsible for the long-term presence of myofibroblasts. A recent study by Marino et al. used the Pseudomonas corneal infection model and found that the EBM completely regenerated and myofibroblasts disappeared in the anterior stroma, while myofibroblasts persisted in the posterior stroma, where the DM and endothelium were damaged [17]. Thus, our results support previous findings that EBM plays a critical role in modulating myofibroblast development and stromal fibrosis by regulating the infiltration of TGF-β1. Damage to the DM and endothelium may lead to sustained posterior stromal fibrosis.

We detected TGF-β1 in the stroma in this corneal perforating injury model. It was likely that TGF-β1 was expressed by the infiltrating bone marrow-derived cells and

vimentin-positive corneal fibroblasts, or even the myofibroblasts themselves [13,42]. Alternatively, it is possible that all of the TGF-β1 localized to the stroma was derived from tear, epithelium, and aqueous humor, and what was detected was TGF-β1 bound to receptors on corneal fibroblasts and other stromal cells [13,14,43-45]]. Further studies are needed to confirm the exact sources of TGF-β1.

The persistence of posterior α-SMA staining in our study indicates persistent injury to the DM and the endothelium after perforating injury. Similar findings were reported by Medeiros et al. and Sampaio et al. [24,36]. Both used the same model (Descemet's membrane-endothelial excision in rabbits) to study posterior stromal fibrosis. They found that the α-SMA positive myofibroblasts persisted in the posterior stroma, where there were no DM and endothelium. Sampaio et al. extended the observation time and found that α-SMA positive myofibroblasts disappeared in the posterior region when the DM and endothelium were regenerated [36]. The persistence of α-SMA positive myofibroblasts are dependent on the ongoing supply of TGF-β1, while the real cause of TGF-β1 persistence in the posterior stroma remains uncertain. Defective DM regeneration might be a factor in high levels of TGF-β1 from the aqueous humor entering the posterior stroma. Accordingly, promoting the regeneration of DM and the reduction of TGF-β1 may be helpful for anti-scarring therapy of corneal perforating injury.

In conclusion, EBM regeneration occurs earlier than DM following corneal perforating injury. TGF-β1 and α-SMA exhibit similar temporal and spatial expression patterns. During the early stages, TGF-β1 and α-SMA are distributed throughout the entire healing stroma, showing decreasing expression from the anterior to the posterior region. Regeneration of EBM may contribute to decreased corneal scarring. Defective regeneration of DM may account for the presence of TGF-β1 and α-SMA in the posterior stroma. However, future studies are warranted to identify the sources of the TGF-β1 and the factors that affect DM regeneration and posterior stromal fibrosis.

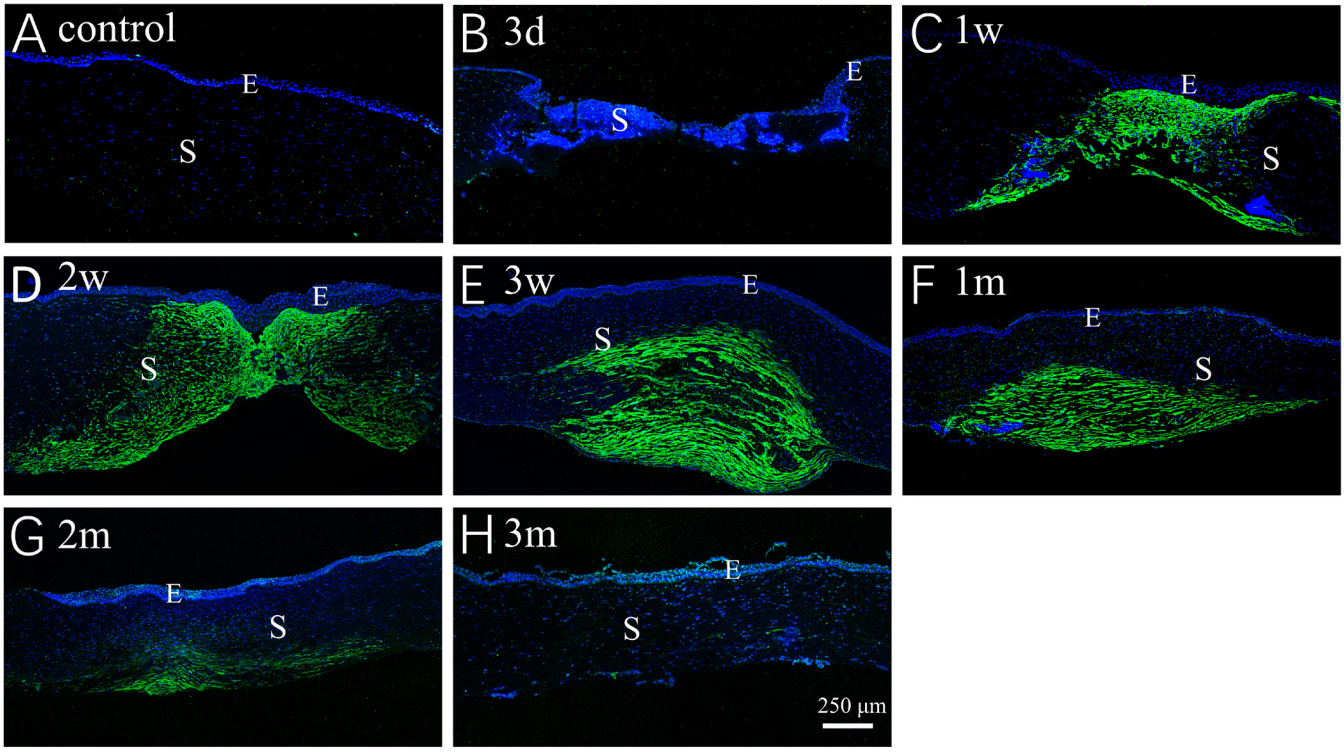

Figure 4. Immunofluorescence staining for α-SMA in fibrotic healing corneas at different time points. **A**: Control cornea exhibited no α-SMA staining. **B**: At 3 days after injury, no α-SMA staining was observed. **C**: At 1 week after injury, α-SMA had appeared in the most anterior stroma. **D**: At 2 weeks after injury, α-SMA had appeared in the entire repairing stroma. **E**: At 3 weeks after injury, α-SMA had appeared in the most posterior stroma. **F-G**: At 1 to 2 months after injury, α-SMA was detected in the posterior stroma, and the positively stained area for α-SMA had reduced. **H**: At 3 months after injury, α-SMA staining was nearly absent in the wound stroma. Green staining indicates α-SMA protein. Blue is DAPI staining of cell nuclei. (E) is the epithelium, and (S) is the stroma. Magnification: ×100. Scale bar: 250 μm.

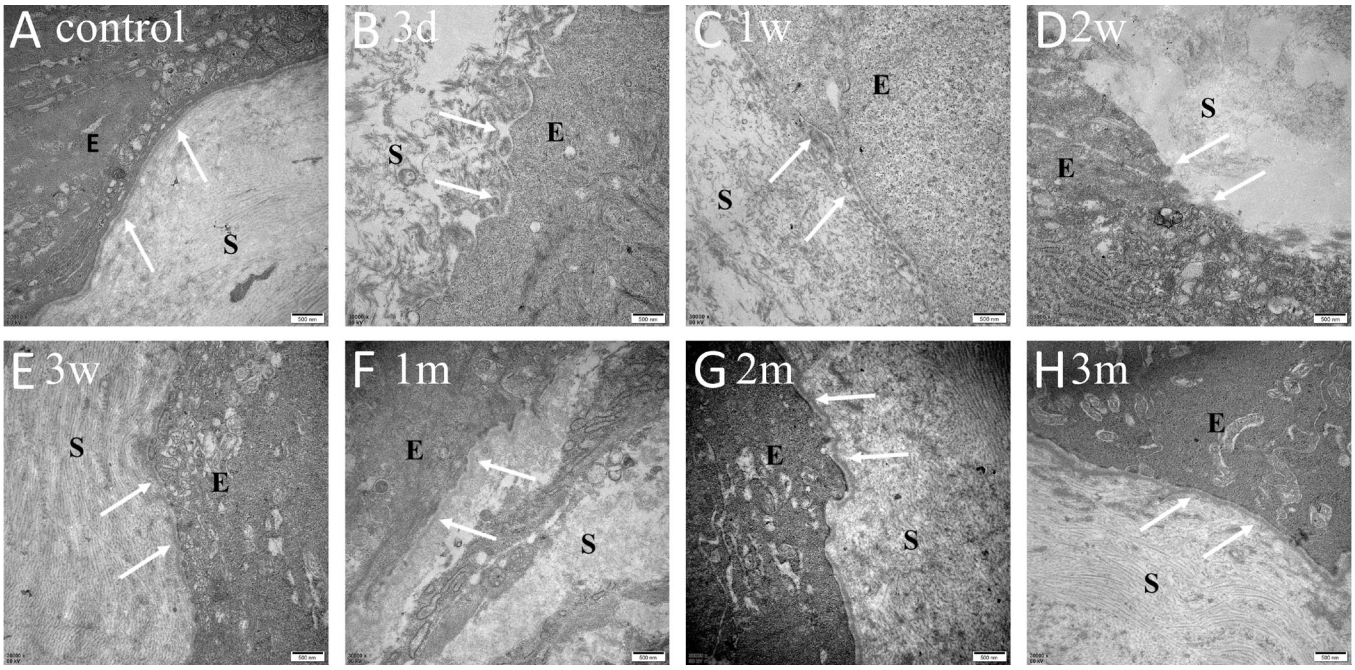

Figure 5. Epithelial basement membrane (EBM) regeneration at different time points in rabbit corneas (scale bar: 500 nm, magnification: ×30,000). A: Unwounded (control) corneas had normal EBM ultrastructure with lamina lucida and lamina densa. B–D: After perforating injury, all corneas at 3 days to 2 weeks showed no evidence of regeneration of lamina lucida and lamina densa. E: Three weeks after injury, a nascent defective EBM was first observed, and the lamina lucida and lamina densa were irregular and discontinuous. F: One month after injury, the EBM ultrastructure was somewhat restored, but its ultrastructural morphology was still uncontinuous. G: Two months after injury, the EBM lamina lucida and lamina densa showed more continuity, and there were a few discontinuous EBM ultrastructures. H: Three months after injury, continuous and regular lamina lucida and lamina densa were noted, and EBM was nearly fully regenerated. Arrows indicate the lamina densa and lamina lucida of the epithelial basement membrane. **A** represents the control cornea. **B**–**H** represent injured corneas. (E) is the epithelium. (S) is the stroma.

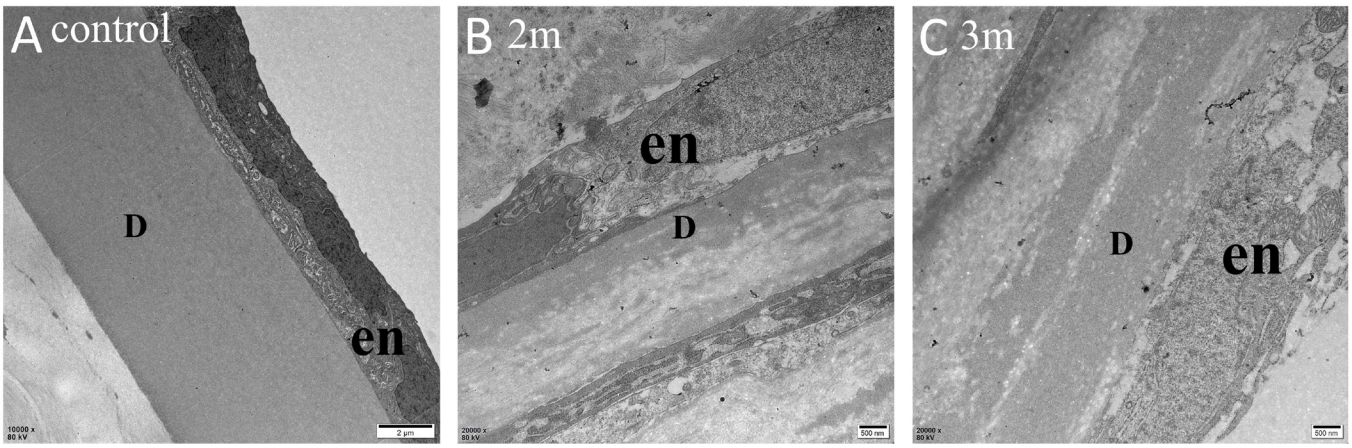

Figure 6. Descemet's membrane (DM) regeneration at different time points in rabbit corneas. A: In the normal cornea, DM was thick and even (scale bar: 2μm, magnification: ×10,000). B: At 2 months after injury, a thin DM first appeared in the posterior stroma near the nascent endothelium (scale bar: 500 nm, magnification: ×20,000). C: At 3 months after injury, thicker but uneven DM appeared in the posterior stroma adjacent to the endothelium. (en) represents the endothelial cell. (D) indicates Descemet's membrane.

ACKNOWLEDGMENTS

This work was supported by the National Natural Science Foundation of China (Grant number 81,360,144, China) and the Natural Science Foundation of Guangxi Province (Grant number 2017GXNSFAA198250, Guangxi, China). No author has a financial or proprietary interest in any material or method mentioned. Na Meng and Jinling Wu contributed equally to the conduct of this research and are considered to be co-first authors.

REFERENCES

1. Medeiros CS, Marino GK, Santhiago MR, Wilson SE. The Corneal Basement Membranes and Stromal Fibrosis. Invest Ophthalmol Vis Sci 2018; 59:4044-53. [PMID: 30098200].
2. Wilson SE, Torricelli AAM, Marino GK. Corneal epithelial basement membrane: Structure, function and regeneration. Exp Eye Res 2020; 194:108002-[PMID: 32179076].
3. de Oliveira RC, Wilson SE. Descemet's membrane development, structure, function and regeneration. Exp Eye Res 2020; 197:108090-[PMID: 32522478].
4. Wilson SE. Coordinated Modulation of Corneal Scarring by the Epithelial Basement Membrane and Descemet's Basement Membrane. J Refract Surg 2019; 35:506-16. [PMID: 31393989].
5. Wilson SE. Fibrosis Is a Basement Membrane-Related Disease in the Cornea: Injury and Defective Regeneration of Basement Membranes May Underlie Fibrosis in Other Organs. Cells 2022; 11:309-[PMID: 35053425].
6. Saika S. TGF beta pathobiology in the eye. Lab Invest 2006; 86:106-15. [PMID: 16341020].
7. Tandon A, Tovey JCK, Sharma A, Gupta R, Mohan RR. Role of Transforming Growth Factor Beta in Corneal Function, Biology and Pathology. Curr Mol Med 2010; 10:565-78. [PMID: 20642439].
8. Lichtman MK, Otero-Vinas M, Falanga V. Transforming growth factor beta (TGF-beta) isoforms in wound healing and fibrosis. Wound Repair Regen 2016; 24:215-22. [PMID: 26704519].
9. Wilson SE. TGF beta-1,-2 and-3 in the modulation of fibrosis in the cornea and other organs. Exp Eye Res 2021; 207:108594-[PMID: 33894227].
10. Jester JV, Brown D, Pappa A, Vasiliou V. Myofibroblast Differentiation Modulates Keratocyte Crystallin Protein Expression, Concentration, and Cellular Light Scattering. Invest Ophthalmol Vis Sci 2012; 53:770-8. [PMID: 22247459].
11. Jester JV, Huang JY, Petroll WM, Cavanagh HD. TGF beta induced myofibroblast differentiation of rabbit keratocytes requires synergistic TGF beta, PDGF and integrin signaling. Exp Eye Res 2002; 75:645-57. [PMID: 12470966].
12. Jester JV, Huang JY, Barry-Lane PA, Kao WWY, Petroll WM, Cavanagh HD. Transforming growth factor(beta)-mediated corneal myofibroblast differentiation requires actin and fibronectin assembly. Invest Ophthalmol Vis Sci 1999; 40:1959-67. [PMID: 10440249].
13. de Oliveira RC, Tye G, Sampaio LP, Shiju TM, DeDreu J, Menko AS, Santhiago MR, Wilson SE. TGF beta 1 and TGF beta 2 proteins in corneas with and without stromal fibrosis: Delayed regeneration of apical epithelial growth factor barrier and the epithelial basement membrane in corneas with stromal fibrosis. Exp Eye Res 2021; 202:108325-[PMID: 33263285].
14. Wilson SE. Interleukin-1 and Transforming Growth Factor Beta: Commonly Opposing, but Sometimes Supporting, Master Regulators of the Corneal Wound Healing Response to Injury. Invest Ophthalmol Vis Sci 2021; 62:8-[PMID: 33825855].
15. Torricelli AAM, Santhanam A, Wu JH, Singh V, Wilson SE. The corneal fibrosis response to epithelial-stromal injury. Exp Eye Res 2016; 142:110-8. [PMID: 26675407].
16. Torricelli AAM, Singh V, Agrawal V, Santhiago MR, Wilson SE. Transmission Electron Microscopy Analysis of Epithelial Basement Membrane Repair in Rabbit Corneas With Haze. Invest Ophthalmol Vis Sci 2013; 54:4026-33. [PMID: 23696606].
17. Marino GK, Santhiago MR, Santhanam A, Lassance L, Thangavadivel S, Medeiros CS, Bose K, Tam KP, Wilson SE. Epithelial basement membrane injury and regeneration modulates corneal fibrosis after pseudomonas corneal ulcers in rabbits. Exp Eye Res 2017; 161:101-5. [PMID: 28506643].
18. Marino GK, Santhiago MR, Santhanam A, Torricelli AAM, Wilson SE. Regeneration of Defective Epithelial Basement Membrane and Restoration of Corneal Transparency After Photorefractive Keratectomy. J Refract Surg 2017; 33:337-46. [PMID: 28486725].
19. Connon CJ, Meek KM. Organization of corneal collagen fibrils during the healing of trephined wounds in rabbits. Wound Repair Regen 2003; 11:71-8. [PMID: 12581429].
20. Fantes FE, Hanna KD, Waring GO 3rd, Pouliquen Y, Thompson KP, Savoldelli M. Wound healing after excimer laser keratomileusis (photorefractive keratectomy) in monkeys. Arch Ophthalmol 1990; 108:665-75. [PMID: 2334323].
21. Torricelli AAM, Wilson SE. Cellular and extracellular matrix modulation of corneal stromal opacity. Exp Eye Res 2014; 129:151-60. [PMID: 25281830].
22. Mukhija R, Gupta N, Vashist P, Tandon R, Gupta SK. Population-based assessment of visual impairment and pattern of corneal disease: results from the CORE (Corneal Opacity Rural Epidemiological) study. Br J Ophthalmol 2020; 104:994-8. [PMID: 31628205].
23. Santhanam A, Marino GK, Torricelli AA, Wilson SE. EBM regeneration and changes in EBM component mRNA expression in stromal cells after corneal injury. Mol Vis 2017; 23:39-51. [PMID: 28275314].

24. Medeiros CS, Saikia P, de Oliveira RC, Lassance L, Santhiago MR, Wilson SE. Descemet's Membrane Modulation of Posterior Corneal Fibrosis. Invest Ophthalmol Vis Sci 2019; 60:1010-20. [PMID: 30884531].
25. Wilson SE, Sampaio LP, Shiju TM, Hilgert GSL, de Oliveira RC. Corneal Opacity: Cell Biological Determinants of the Transition From Transparency to Transient Haze to Scarring Fibrosis, and Resolution, After Injury. Invest Ophthalmol Vis Sci 2022; 63:22-[PMID: 35044454].
26. Hu B, Wu Z, Phan SH. Smad3 mediates transforming growth factor-beta-induced alpha-smooth muscle actin expression. Am J Respir Cell Mol Biol 2003; 29:397-404. [PMID: 12702545].
27. Meng XM, Nikolic-Paterson DJ, Lan HY. TGF-beta: the master regulator of fibrosis. Nat Rev Nephrol 2016; 12:325-38. [PMID: 27108839].
28. Rocher M, Robert PY, Desmouliere A. The myofibroblast, biological activities and roles in eye repair and fibrosis. A focus on healing mechanisms in avascular cornea. Eye (Lond) 2020; 34:232-40. [PMID: 31767967].
29. Wilson SE. Corneal myofibroblasts and fibrosis. Exp Eye Res 2020; 201:108272-[PMID: 33010289].
30. Xu LX, Wu JL, Wang SN, Li X. Procedure for early corneal basement membrane repair and regeneration in corneal penetrating injury in rabbits. Chinese Journal of Experimental Ophthalmology 2020; 38:93-9. .
31. Yurchenco PD, Tsilibary EC, Charonis AS, Furthmayr H. Models for the self-assembly of basement membrane. J Histochem Cytochem 1986; 34:93-102. [PMID: 3510247].
32. Yurchenco PD, Patton BL. Developmental and Pathogenic Mechanisms of Basement Membrane Assembly. Curr Pharm Des 2009; 15:1277-94. [PMID: 19355968].
33. Wilson SE. Defective perlecan-associated basement membrane regeneration and altered modulation of transforming growth factor beta in corneal fibrosis. Cell Mol Life Sci 2022; 79:144-[PMID: 35188596].
34. Torricelli AA, Marino GK, Santhanam A, Wu J, Singh A, Wilson SE. Epithelial basement membrane proteins perlecan and nidogen-2 are up-regulated in stromal cells after epithelial injury in human corneas. Exp Eye Res 2015; 134:33-8. [PMID: 25797478].
35. Santhanam A, Torricelli AA, Wu J, Marino GK, Wilson SE. Differential expression of epithelial basement membrane components nidogens and perlecan in corneal stromal cells in vitro. Mol Vis 2015; 21:1318-27. [PMID: 26788024].
36. Sampaio LP, Shiju TM, Hilgert GSL, de Oliveira RC, DeDreu J, Menko AS, Santhiago MR, Wilson SE. Descemet's membrane injury and regeneration, and posterior corneal fibrosis, in rabbits. Exp Eye Res 2021; 213:108803-[PMID: 34736886].
37. Vercammen H, Miron A, Oellerich S, Melles GRJ, Dhubhghaill SN, Koppen C, Bogerd BV. Corneal endothelial wound healing: understanding the regenerative capacity of the innermost layer of the cornea. Transl Res 2022; 248:111-27. [PMID: 35609782].
38. Joyce NC. Cell cycle status in human corneal endothelium. Exp Eye Res 2005; 81:629-38. [PMID: 16054624].
39. West-Mays JA, Dwivedi DJ. The keratocyte: Corneal stromal cell with variable repair phenotypes. Int J Biochem Cell Biol 2006; 38:1625-31. [PMID: 16675284].
40. de Oliveira RC, Wilson SE. Fibrocytes, Wound Healing, and Corneal Fibrosis. Invest Ophthalmol Vis Sci 2020; 61:28-[PMID: 32084275].
41. Kim KK, Sheppard D, Chapman HA. TGF-β1 Signaling and Tissue Fibrosis. Cold Spring Harb Perspect Biol 2018; 10:a022293-[PMID: 28432134].
42. Lassance L, Marino GK, Medeiros CS, Thangavadivel S, Wilson SE. Fibrocyte migration, differentiation and apoptosis during the corneal wound healing response to injury. Exp Eye Res 2018; 170:177-87. [PMID: 29481786].
43. Gupta A, Monroy D, Ji Z, Yoshino K, Huang A, Pflugfelder SC. Transforming growth factor beta-1 and beta-2 in human tear fluid. Curr Eye Res 1996; 15:605-14. [PMID: 8670763].
44. Lee JB, Choe CM, Kim HS, Seo KY, Seong GJ, Kim EK. Comparison of TGF-beta1 in tears following laser subepithelial keratomileusis and photorefractive keratectomy. J Refract Surg 2002; 18:130-4. [PMID: 11934200].
45. Cousins SW, McCabe MM, Danielpour D, Streilein JW. Identification of transforming growth factor-beta as an immunosuppressive factor in aqueous humor. Invest Ophthalmol Vis Sci 1991; 32:2201-11. [PMID: 2071334].

Articles are provided courtesy of Emory University and the Zhongshan Ophthalmic Center, Sun Yat-sen University, P.R. China. The print version of this article was created on 20 May 2023. This reflects all typographical corrections and errata to the article through that date. Details of any changes may be found in the online version of the article.